Dedicated to innovation in aerospace

NLR-TP-2021-313 | October 2021

Development of Magnesium Laser Powder Bed Fusion to manufacture light-weight components for Vertical Lift applications

CUSTOMER: Boeing

Royal NLR - Netherlands Aerospace Centre

Dedicated to innovation in aerospace

Development of Magnesium Laser Powder Bed Fusion to manufacture light-weight components for Vertical Lift applications

Problem area

The objective of the research project, described in this paper, is to demonstrate the capability to produce high quality magnesium transmission housings with high complexity by Laser Powder Bed Fusion (LPBF).

Description of work

A first step in the development was the selection of a metal powder with adequate spreadability for LPBF. An efficient optimization approach was applied that enabled the selection of process parameters by analysis of an array of thin wall and block samples from one single build job. After the process parameter selection, benchmark parts were produced for evaluating design rules to print magnesium parts. Demonstrator parts were successfully produced based on a representative light-weight component for Vertical Lift applications.

REPORT NUMBER
NLR-TP-2021-313

AUTHOR(S)
M.J. de Smit
M.L. Montero-Sistiaga
L. 't Hoen-Velterop
A. Paesano

REPORT CLASSIFICATION
UNCLASSIFIED

DATE
October 2021

KNOWLEDGE AREA(S)
Aerospace Materials

DESCRIPTOR(S)
Metal AM
Additive Manufacturing
Selective Laser Melting
SLM
Magnesium

Results and conclusions

The following conclusions are drawn from this study.

- The evaluation of the magnesium powder that was used in this study indicated that a good processability could be expected for LPBF.
- An efficient optimization approach was applied that enabled selection of LPBF process parameters for the production of low porosity and roughness parts.
- Scanning electron microscopy analysis showed a homogeneous microstructure at the melt pool and grain size scale. Some Y and Nd-rich precipitates were observed, which are typical for alloy WE43.
- LPBF of alloy WE43 results in very fine equiaxed grains, homogeneously distributed across the melt-pools.
- Some deformation occurred due to residual stresses. It is recommended to take the formation of residual stresses into account when designing parts and supports structures for LPBF of magnesium.
- No optimized heat treatment is available for printed magnesium material. It is recommended to develop a dedicated heat treatment for LPBF processed magnesium to obtain the required mechanical performance, corrosion resistance and minimum risk of deformation.
- It is recommended to determine elastic, plastic and thermal expansion properties of LPBF magnesium material for the simulation of deformations in order to evaluate and optimize the design and the support structures.

Applicability

Magnesium is the lightest of all structural metals. It also possesses mechanical strength, fatigue resistance, a ratio of elastic modulus/density almost equal to that of aluminium, shock resistance, strong thermo-conductivity and electromagnetic shielding. As a result, magnesium alloys are attractive in various applications like aerospace, automotive, missiles, projectiles, construction, electronic, powertrain, and military.
Aviation is especially interested in magnesium, because it enables to reduce weight, hence, thereby reducing emissions and increasing fuel efficiency, without penalizing strength and stiffness. LPBF makes it possible to reduce weight and improve the performance of parts compared to conventionally produced components. These advantages are especially beneficial for aerospace applications, such as in vertical lift applications.

GENERAL NOTE
This report is based on a presentation held at the Vertical Flight System (VFS) Forum, West Palm Beach (USA)-Virtual, 11-13 May 2021..

Royal NLR
Anthony Fokkerweg 2
1059 CM Amsterdam, The Netherlands
p) +31 88 511 3113
e) info@nlr.nl i) www.nlr.nl

Dedicated to innovation in aerospace

NLR-TP-2021-313 | October 2021

Development of Magnesium Laser Powder Bed Fusion to manufacture light-weight components for Vertical Lift applications

CUSTOMER: Boeing

AUTHOR(S):

M.J. de Smit	NLR
M.L. Montero-Sistiaga	NLR
L. 't Hoen-Velterop	NLR
A. Paesano	Boeing

Royal NLR - Netherlands Aerospace Centre

This report is based on a presentation held at the Vertical Flight System (VFS) Forum, West Palm Beach (USA)-Virtual, 11-13 May 2021.Vertical Flight System (VFS) Forum, West Palm Beach (USA)-Virtual, 11-13 May 2021.

CUSTOMER	**Boeing**
CONTRACT NUMBER	**1675607**
OWNER	**NLR**
DIVISION NLR	**Aerospace Vehicles**
DISTRIBUTION	**Unlimited**
CLASSIFICATION OF TITLE	**UNCLASSIFIED**

APPROVED BY :		
AUTHOR	**REVIEWER**	**MANAGING DEPARTMENT**
M.J. de Smit M.J. de Smit 2021.10.26 09:33:29 +02'00'	E. Amsterdam Emiel Amsterdam 2021.10.25 17:57:05 +02'00'	H.G.S.J Thuis Digitally signed by H.G.S.J. Thuis Date: 2021.10.26 09:18:45 +02'00'
DATE	DATE	DATE

Abstract

This paper describes the work that was conducted to demonstrate the capability to produce high quality representative magnesium products for vertical lift applications by Laser Powder Bed Fusion (LPBF). An important step in the development was the selection of a metal powder with adequate spreadability for LPBF. Optimum process parameters are required for the production of parts featuring low porosity and low roughness. An efficient optimization approach was applied that enabled the selection of process parameters by analysis of an array of thin wall and block samples from one single build job. After the process parameter selection, benchmark parts were produced for evaluating design rules to print magnesium parts. Demonstrator parts were successfully produced based on a representative light-weight component for Vertical Lift applications. A very fine homogeneous microstructure was found at the melt-pool and grain size scale. After the removal of the parts from the baseplate, some deformation occurred due to residual stresses.

Contents

Abbreviations

ACRONYM	DESCRIPTION
AM	Additive Manufacturing
EBSD	Electron backscatter diffraction
ECAP	Equal-channel angular pressing
EDX	Energy Dispersive X-ray
HIP	Hot Isostatic Pressing
LPBF	Laser Powder Bed Fusion
LZH	Laser Zentrum Hannover
OM	Optical Microscopy
PSD	Particle Size Distribution
SEM	Scanning Electron Microscope

1 Introduction

Laser Powder Bed Fusion (LPBF) is an Additive Manufacturing (AM) process that creates fully dense components starting from metal powder particles. First, a 3D model is numerically sliced in 2D layers and a laser scan pattern is generated for each layer. Secondly, a thin powder layer is deposited onto the build platform and then the laser beam selectively melts the 2D powder layer. Then, the build platform is lowered the same distance as the predefined layer thickness and the next powder layer is deposited. This process is repeated until the 3D component is fully built.
LPBF offers great opportunities thanks to the freedom in design. LPBF makes it possible to reduce weight and improve the performance of parts compared to conventionally produced components. These advantages are especially beneficial for aerospace applications, such as in vertical lift applications. Several materials have already been processed with LPBF, such as: nickel superalloys for high-temperature applications, titanium alloys for low-weight structural applications or AM-aluminium alloys for low-weight parts and thermal applications. Magnesium has been the preferred material for vertical lift transmission casings due to the combination of low density and high specific strength. Magnesium LPBF therefore offers great potential for vertical lift applications. Internal channels for lubrication and/or cooling can be optimized and substantial additional weight reduction can be achieved compared to cast products. However, magnesium is a challenging material to process in LPBF due to its low boiling point and the high reactivity with oxygen.

LPBF processing of magnesium has been investigated by several researchers. Most interest in magnesium AM has come from the biomedical field. This is because magnesium is a potential implant material for biodegradable applications as described by Jauer et al. [Ref. 1]. The first investigations on magnesium LPBF were published in 2009 by Ng et al. [Ref. 2], [Ref. 3]. Single tracks were made by Ng out of a pure magnesium powder with a pulsed Nd:YAG laser in a shielding argon gas atmosphere. Ng et al. [Ref. 4] further investigated magnesium processing under different processing conditions using the same setup and continuous wave irradiation. Tracks with disrupted surfaces and regular beads were produced whereas pulsed mode irradiation led to a flat surface morphology with pores within the track. The main challenges for AM of magnesium were addressed in these studies: the high oxygen affinity, the minimal difference between melt and vaporization temperature of magnesium, and the evaporation of alloy constituents.
Zhang et al. [Ref. 5] investigated LPBF of Mg–9%Al powder mixture in a commercial LPBF system for the first time in 2011. Structures with a relative density of 82% were produced. In 2012, Jauer et al. [Ref. 1] carried out initial studies on the development of LPBF of magnesium for medical applications with magnesium AZ91 alloy. Test specimens with a density > 99% were built.
Gieseke et al. [Ref. 6], [Ref. 7] investigated LPBF of magnesium alloys at the Laser Zentrum Hannover (LZH) for the production of biodegradable implants. LZH worked with ATOULTRA 325 pure magnesium powder and with a biocompatible MgCa0.8 alloy. Gieseke et al. [Ref. 6], [Ref. 7] observed substantial evaporation and black deposits. The depositions appeared to be nanosized alloy components and oxides. A customized LPBF system was developed by Gieseke et al. [Ref. 6], [Ref. 7] that enabled production at elevated pressure to increase the boiling temperature. It was concluded that the increased pressure was not beneficial for the produced material quality. Increasing the pressure also did not reduce the process emissions.
Esmaily et al. [Ref. 8] recently investigated the microstructure and corrosion behaviour of additively manufactured magnesium. Samples were produced out of Mg alloy WE43 by LPBF. The influence of hot isostatic pressing (HIP) and an additional solution heat treatment were investigated. The microstructure was compared to conventional cast alloy counterparts. The authors found that the LPBF material had a unique fine-grained microstructure with a strong crystallographic texture. A low fraction of process-induced and metallurgical defects were found after the HIP treatment. The LPBF material was found to be cathodically more active compared to conventionally cast material.

Esmaily et al. recommend further investigation of the influence of powder characteristics on the corrosion resistance of LPBF Mg alloys.

This paper describes work that has been carried out in collaboration with Boeing to demonstrate the capability to produce good quality representative magnesium products for vertical lift applications by LPBF. The goal of Boeing in pursuing additive manufacturing of magnesium is exploiting its high specific strength and stiffness, and other advantageous properties combined with design freedom resulting in enhanced performance and functionality.

2 Opportunities of magnesium additive manufacturing in vertical lift applications

Magnesium is the lightest of all structural metals with a density (g/cm^3) of 1.74 compared to 2.70 for aluminium, and 7.87 for iron. Since magnesium also possesses mechanical strength, fatigue resistance, a ratio of elastic modulus/density almost equal to that of aluminium (24 vs. 26), shock resistance, strong thermo-conductivity and electromagnetic shielding, magnesium alloys are attractive in various applications like aerospace, automotive, missiles, projectiles, construction, electronic, powertrain, and military [Ref. 9].

Aviation is especially interested in magnesium, because it enables to reduce weight, hence, thereby reducing emissions and increasing fuel efficiency, without penalizing strength and stiffness. This interest goes back to the 1940's [Ref. 10]. Lately, magnesium has benefited from enhanced properties exceeding those of aluminium [Ref. 11], corrosion resistance improved up to 60 times, and new forging processes that cut the costs of manufacturing secondary fuselage components, such as panels of internal inspection doors, and window frames, and met the mechanical requirements for aluminium articles [Ref. 12].

The suitability of magnesium for aviation components is also demonstrated by the fact that research programs have received the financial support of major companies and organizations such as Airbus, Airbus Helicopters, Alenia, EADS Deutschland, Israel Aviation Industry, and Liebherr-Aerospace [Ref. 13]. Current established technologies for magnesium like forging, casting, and equal-channel angular pressing (ECAP) are limited by risk of ignition upon machining, ageing process (lowering mechanical performance), and restrictions in achieving complex shapes. New technologies for magnesium are backward extrusion and Kobo extrusion. AM addresses one of the above limitations by greatly increasing design freedom [Ref. 13], which in turn enables to reduce weight without sacrificing structural performance by leveraging topological optimization.

Several aviation parts in magnesium have been studied and fabricated, and include flat, ribbed, and contoured articles, and even critically loaded parts. Examples of magnesium parts produced by closed-die forging, and deep drawing are compressor wheels, impellers with twisted blades, compressor upper cases, antenna supports, window frames, door stop fittings [Ref. 14] and wheel hubs [Ref. 15]. The unmanned ILX-27 is a classic helicopter construction with a single, three blade main rotor, a ducted fan tail and the piston engine. Its control system comprises levers that are heavily loaded. The original levers, forged in aluminium P7 (corresponding to aluminium 2024), were replaced with versions in magnesium AZ31B. A weight reduction of 35% was achieved. The magnesium levers passed a 100 h fatigue test, although tensile ultimate and yield strength of AZ31B are 230 MPa and 150 MPa, respectively, and for PA 7 are 360–435 MPa and 250–290, respectively [Ref. 16]. In helicopters, controls comprise brackets in various locations: control stick, electric elements, spring mechanisms, transverse control pushers, longitudinal control pushers, and hydraulic amplifiers [Ref. 17]. Ribbed brackets in AZ31 magnesium alloy were forged according to a newly developed process and were successfully tested [Ref. 18]. Aviation demonstrator parts in magnesium include door hinges and shelf removal assemblies that were 52% and 20% lower in weight, respectively in comparison to their original alloy [Ref. 13].

3 Materials and methods

3.1 Powder characterization

In this work, Magnesium alloy WE43 was selected to manufacture light-weight components for Vertical Lift applications by LPBF. This is a casting alloy with good mechanical properties at both ambient and elevated temperatures and with good corrosion resistance. The composition of this alloy is shown in Table 1. A sieve fraction of 20-63 µm (-230/+635 mesh) was selected for this study.

Table 1 Magnesium WE43 powder composition

Element	Weight percent [%]
Magnesium	Bal.
Yttrium	3.7-4.3
Zirconium	0.4-1.0
Zinc	0.2
Manganese	0.15
Coper	0.03
Iron	0.01
Silicon	0.01
Rare Earths	2.4-4.4
Other	0.4

The metal powder is applied in very thin layers in LPBF. Powder properties, application speed, and applicator design determine the density and uniformity of the powder layer. Powder properties also influence how the laser interacts with the powder layer when particles are fused together to a dense material. The morphology and the spreadability of the used power are therefore investigated.

A FEI Nova NanoSEM 450 scanning electron microscope (SEM) was used for analysing the powder particle size distribution (PSD) and morphology. The SEM is equipped with an energy dispersive analysis of X-rays (EDX) detector. The powder is first dispersed over an SEM stub with adhesive carbon using a compressed air burst of 2 bar. Scandium image analysis software and MATLAB were used for analysing the SEM images.

The spreadability of the powder was measured using the in-house SpreadChecker tool. This is a simple method to evaluate the powder behaviour in thin layer application. A small quantity of powder with a known weight is applied on a roughened surface. An applicator is used to spread a thin layer along a ruler with a layer thickness of 100µm. The track length is measured and the layer volume is calculated from the thickness, width and layer length. The powder layer density is calculated from the sample weight and layer volume. The flowability in thin layer application is judged based on the layer density and the thin layer quality. A low density or an irregular layer with stripes indicates bad spreadability behaviour.

3.2 LPBF production

For the production of the parts, an SLM® 280^{HL} (SLM Solutions, Germany) machine was used. It was observed that there were considerably more fumes generated during LPBF processing of magnesium alloy than for AlSi10Mg or Ti-6Al-4V. These fumes consist of nanosized particles which can absorb or deflect the laser beam, resulting in an unstable process. An inert gas flow is used to remove fumes from the melt-pool. The original inert gas flow configuration of the SLM® 280^{HL} machine was not capable of removing all fumes from the process area. Therefore, the inert gas flow configuration was improved so that the extraction of fumes is made more effective. This improvement was found to be an important step in making LPBF processing of magnesium possible. This configuration allows having a laminar flow in the chamber and better fume/spatter removal with minimum recirculation.
During the production, firstly, LPBF process parameters were generated for the contour and bulk parameters. For that purpose, an internally developed parameter optimization procedure was used which allows the production of single walls, for the contour parameter optimization, and blocks with variable hatch spacing, for the bulk parameter optimization. For the optimization of contour parameters, a total of 120 walls were produced with varying speed (300-800 mm/s) and laser power (80-300 W). The 24 variable hatch blocks were produced, each block with a different scan speed (390-710 mm/s) and laser power (90-270 W) combination. Within each block, the hatch spacing was varied from 0.1 to 0.2 mm.
A benchmark part was designed with features that enable determining design guidelines for the magnesium AM demonstrator. Examples of design guidelines are allowable overhang angle and maximum horizontal channel diameter. The benchmark part was designed and produced with the following features (see Figure 1):

1. Large thickness variation.
2. Long shape to investigate the influence of residual stresses.
3. Horizontal channels with diameters 4mm < D < 12 mm.
4. Overhang Angles 30°, 40°, 50°, 60°.
5. Internal 45° roof.
6. One benchmark part is built on supports and one is built directly on the substrate plate.
7. Overall dimensions (length x width x height) are 100 x 33 x 40 mm.

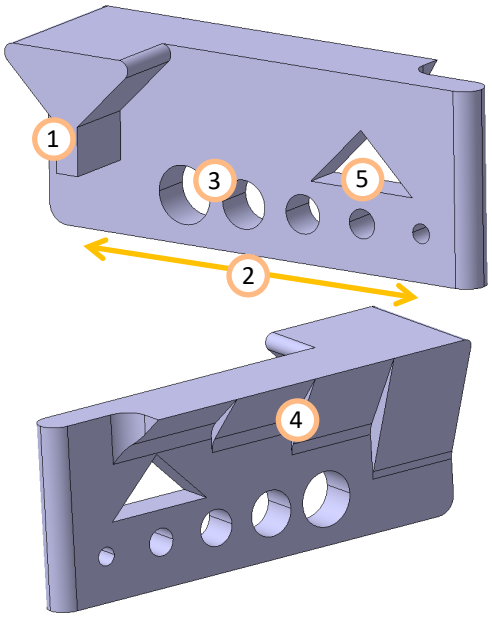

Figure 1: Benchmark part design

A demonstrator design was made based on the original design of a representative light-weight component for Vertical Lift applications, considering the lessons learned from the benchmark part production and evaluation. A 3D geometry scan is made of the third magnesium AM demonstrator part using a GOM Atos 200. The 3D scan is used to compare the printed geometry to the original CAD design. The 3D scan was made after stress-relief treatment, removal from the substrate plate and surface finishing.

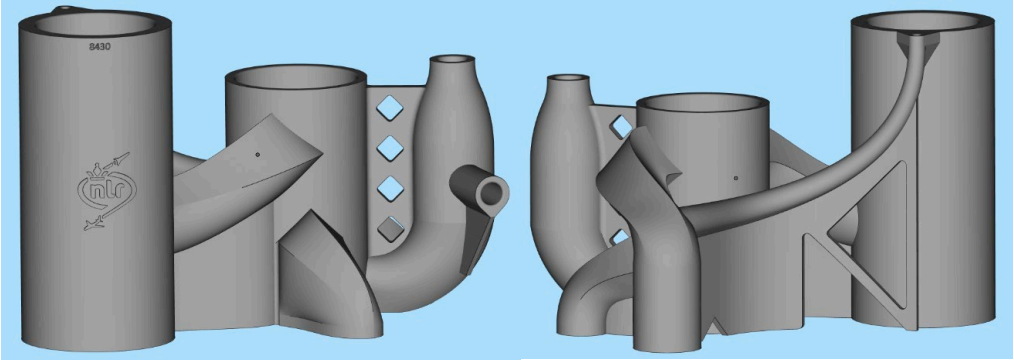

Figure 2: Benchmark part design

The benchmark and demonstrator parts were produced with the optimized parameters, using a linear energy density (E_L) of 0.23 J/mm, which was calculated by dividing the laser power (P) by scan speed (v). In addition, the substrate plate on which the parts were built was preheated to a temperature of 150 °C. The parts were built in an argon atmosphere.
The benchmark and demonstrator parts were heat treated in a circulation oven before removal from the substrate plate. The samples were heated up to 180 °C at a rate of 15 °C/min, holding it for 60 min and air cooling down to room temperature.

3.3 Microstructure analysis

Cross-sections of the parts were used for microstructural analysis and selection of the process parameters.
The samples were ground and polished using Struers OP-S pure suspension. For optical imaging, a Zeiss Axioplan 2 microscope was used. For revealing the microstructure, the cross-sections were etched using 20 ml Acetic acid, 1 ml HNO_3, 60 ml Ethylene Glycol and 20 ml water. The SEM was used for further analysing the microstructure and phase compositions in the microstructure of the parts.

4 Results and discussion

4.1 Powder evaluation

SEM images of the WE43 powder are shown in Figure 3 and Figure 4. As seen in Figure 3, the powder particles are mainly spherical with some small satellite particles attached on the surface. The PSD is analysed from a stitch of 10x10 SEM microscope images (Figure 4). Table 2 shows the D10, D50 and D90 percentile values that indicate the size below which 10%, 50% or 90% of all particles are found respectively. These values are based on measurement of mean diameters in Scanning electron microscope images of WE43 powder.

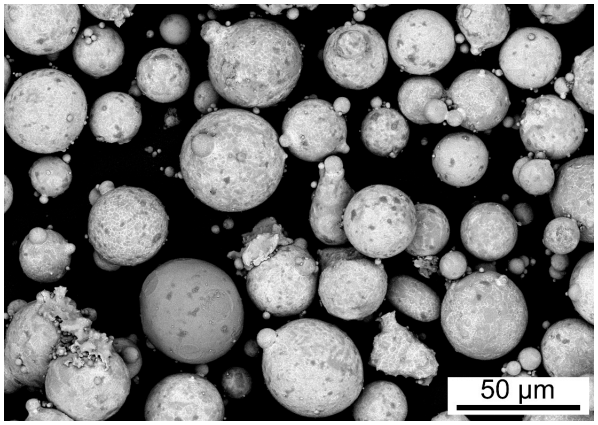

Figure 3: Scanning electron microscope image of WE43 powder.

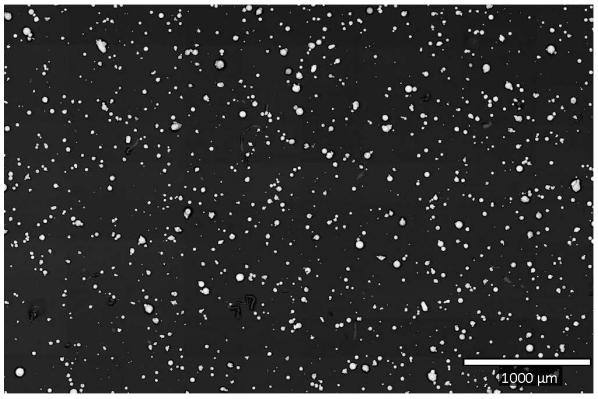

Figure 4: Stitch of 10x10 Scanning electron microscope images of WE43 powder used for the measurement of the particle size and shape

Table 2: D10, D50 and D90 percentile values based on image analysis of Scanning electron microscope images

PSD	Num %	Vol %
D10 [µm]	4.7	25.3
D50 [µm]	23.8	40.1
D90 [µm]	43.6	65.5

The SpreadChecker test was carried out with the magnesium powder. An average layer density of 830 kg/m^3 was measured, which is equal to a relative powder layer density of 46.1%. The applied layers are smooth and without stripes. It is expected that good powder layers can be applied in the LPBF machine.

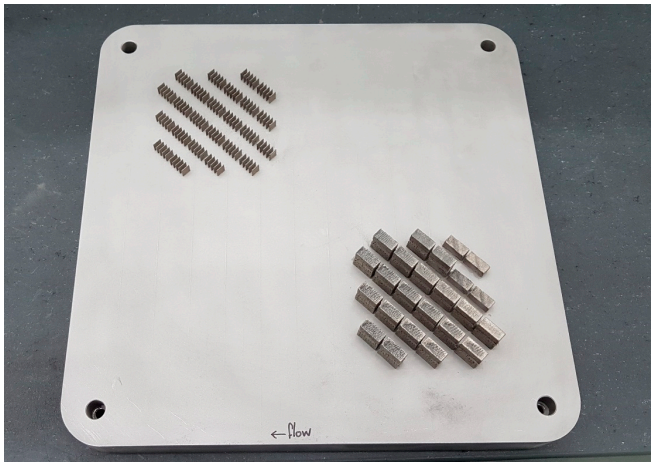

Figure 5: Thin walls and variable hatch blocks built for process parameter optimization

4.2 Development of laser scan parameters for LPBF processing of the SFM WE43 powder

The process parameters for the contour and the bulk area were optimized separately. The contour parameters were selected based on the analysis of thin walls. The bulk parameters were determined by the analysis of building blocks with varying hatch spacing (Figure 5). In order to evaluate the thin walls and the blocks, the cross-sections of these parts were analysed by optical microscope, as shown in Figure 6.

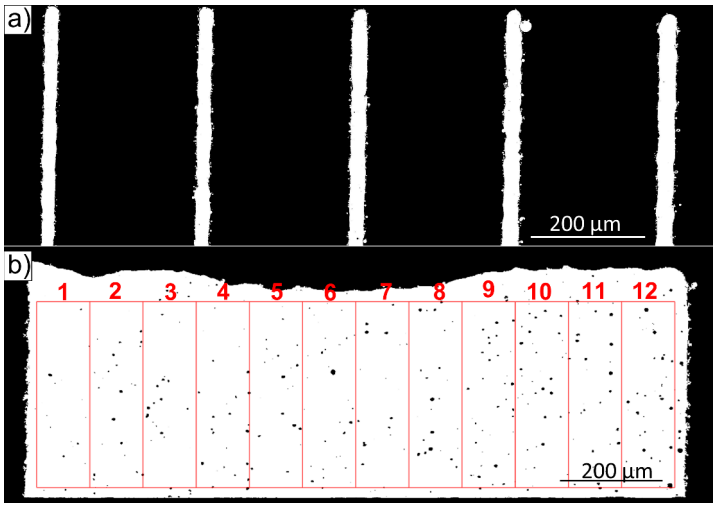

Figure 6: Cross-sections of WE43 a) thin walls and b) variable hatch block

The cross-sections of the thin walls were evaluated on thickness, roughness, and porosity, which were measured using image analysis. The evaluation results of the thin wall cross-sections are shown in Figure 7. In these graphs, the thickness, roughness and porosity of the walls is plotted as function of the applied scan speed v and linear energy density E_L. The average thickness, roughness or porosity of a wall, built with a fixed P and v combination, is presented using a colour scale.

A clear dependence of the wall thickness on the linear energy density is seen as shown in Figure 7-a. The wall thickness increases from around 240 µm at 0.2 J/mm to 360 µm at 0.36 J/mm. It is observed that the roughness shows a slight dependence on the applied scan speed, and not on the energy density (Figure 7-b). Scan speeds below 482 mm/s

result in a roughness below 10 µm. Lastly, the porosity values obtained for all the samples are below 0.4% which suggest a satisfactory consolidation between the layers (Figure 7-c). It was observed that the lowest thin wall porosity was found in walls that were produced with a combination of low energy intensity and low scan speed. A low roughness, low porosity and mid-low thickness is desired, because it will result in high accuracy. The parameter selection is based on these criteria.

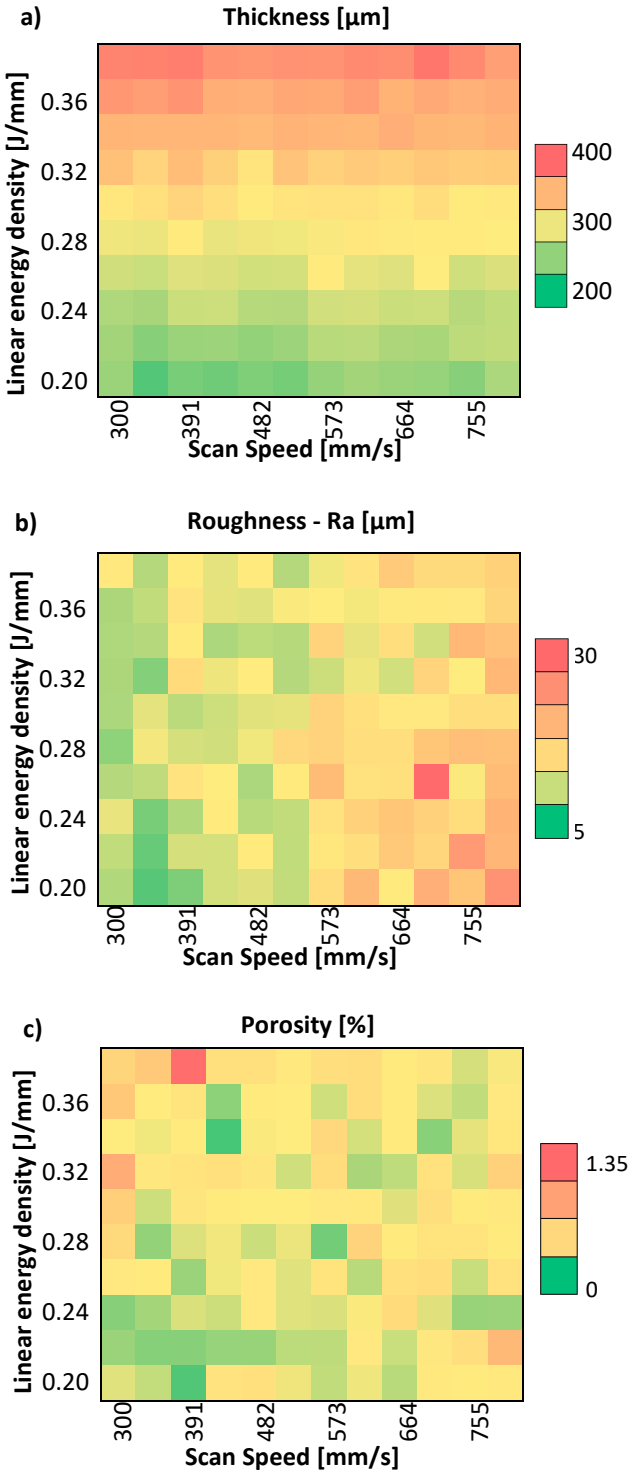

Figure 7: Analysis of the thin wall cross-sections with varying energy density and scan speed for the a) thickness, b) roughness and c) porosity

The cross-sections of the variable hatch blocks are used for analysing the porosity as function of the hatch spacing. A MATLAB script is used for the analysis of the microscope images in the following way. A grey-scale image is converted to black and white using a certain threshold. It is subdivided in a number of equally shaped rectangular fields (for example twelve fields as shown in Figure 6-b). The porosity is calculated in each field by calculating the portion of black pixels compared to the total number of pixels in the area. The results of the porosity analysis of the blocks are shown in Figure 8. Each graph shows the porosity as function of hatch spacing for four different scan speeds. Each colour represents one linear energy density value.

In general, it can be observed that the porosity is dependent on the applied energy input. When increasing the linear energy density (E_L), the porosity increases. A high energy input can lead to keyhole formation which increases the porosity. In addition, the porosity is also influenced by the hatch spacing. When increasing the hatch spacing, the porosity increases. This is caused by the decrease of the overlap between subsequent tracks, which results in lack of fusion pores. A low porosity over a larger hatch spacing range is observed for the higher scan speed values. A low porosity is desired in the bulk. Therefore a low energy input, high scan speed and a relatively small hatch spacing are selected. In this work, a linear energy density (E_L) of 0.23 J/mm was used as optimal parameter set. With this combination, porosities below 0.1% can be obtained which are lower than the ones observed in literature [Ref. 7], [Ref. 8], [Ref. 19].

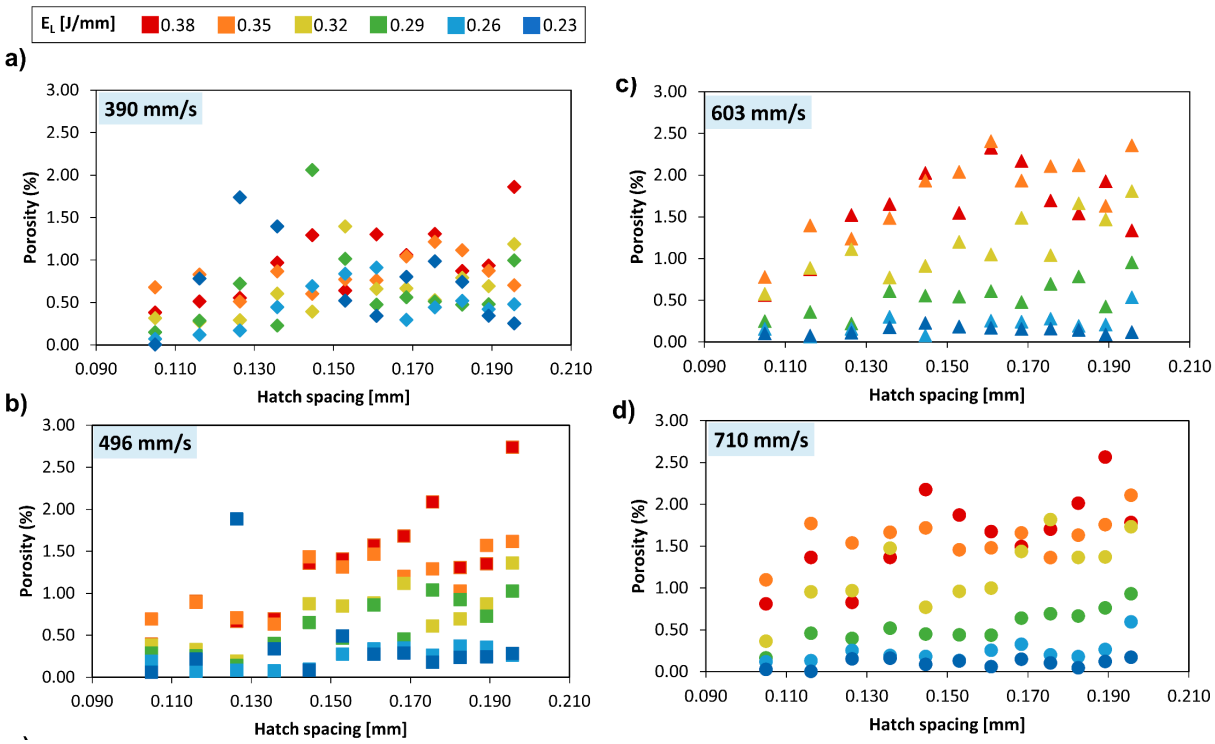

Figure 8: Analysis of the variable hatch blocks' cross-sections plotted as function of the hatch spacing for four different scan speeds: a) 390 mm/s, b) 496 mm/s, c) 603 and d) 710 mm/s. The used energy density for each condition is depicted in the legend

4.3 Production and analysis of benchmark parts

The benchmark parts were successfully produced with the selected process parameters. The as built surface roughness is relatively low and the down facing surfaces are of good quality (see Figure 9). The roughness increases with increasing overhang. One of the benchmark parts was built on a mesh like support structure. A part of the support structure failed due to residual stresses. From this observation can be concluded that residual stresses must be taken into account in the design of the final part and support structures.
Cross-sections of the benchmark parts were investigated by optical microscopy (OM). Figure 10 displays a vertical cross-section. The figure shows a homogeneous structure with low porosity. Some lack of fusion defects are visible in the upper part of the cross-section, as shown in the zoomed inset. The cross-section also shows a good quality down facing surface on the right-hand side of the part.

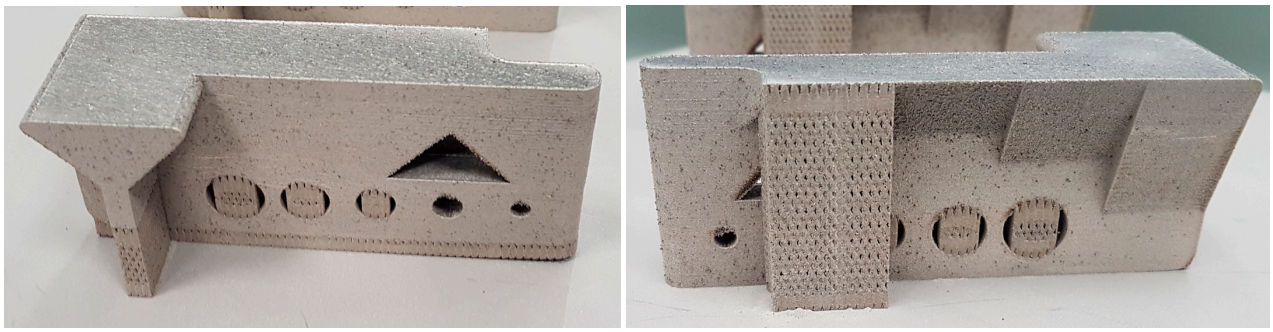

Figure 9: Benchmark parts on substrate plate

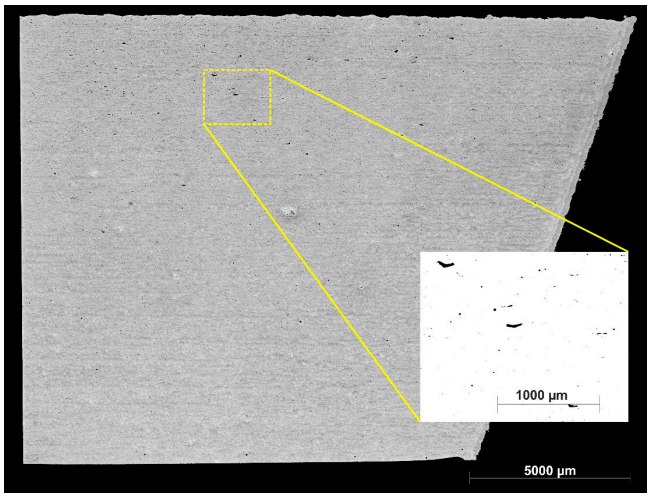

Figure 10: Etched cross-section along the Z direction with an inset of a zoomed un-etched cross-section to show lack of fusion defects

The microstructure was further analysed by SEM and electron backscatter diffraction (EBSD). Figure 11-a shows the microstructure of the cross-section using the backscatter electron detector. The typical LPBF melt-pool structure, highlighted with the orange dashed lines, is observed in Figure 11-a. In addition, some micro-cracks are observed in the cross-sections, as depicted with the blue arrows. These were previously not visible at lower magnification OM images. The size of these micro-cracks is less than 50 µm in length.

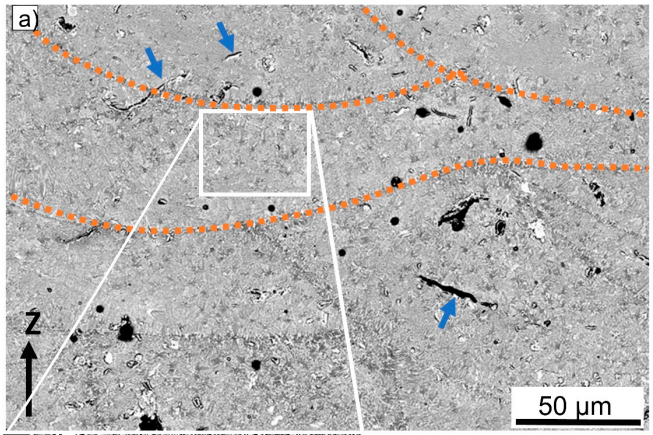

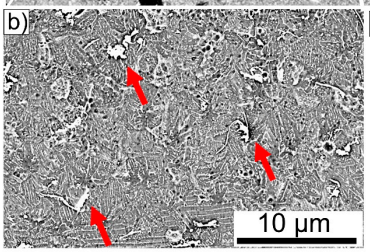

c)

Weight (%)	Matrix	Precipitate
C	7.4	15-16
O	-	13
Mg	86.7	43-45
Y	2.7	20-23
Nd	3.2	5-6

Figure 11: SEM backscatter electron images of the benchmark part parallel to the Z direction (a and b). c) Chemical composition (in weight percentage) of the matrix and the white phases that are highlighted with red arrows in inset b), measured by EDX

A detail of the microstructure inside the melt-pool is shown in Figure 11-b. A very fine cellular-dendritic structure is observed, although the grain boundaries and sub-grain boundaries cannot be distinguished. The red arrows point at the presence of light-coloured precipitates. Their composition as measured by EDX is shown in Figure 11-c. These phases are rich in yttrium and neodymium compared to the matrix composition. It should be noted that the carbon content shown in the table refers to the carbon coating deposited on the cross-section for improved imaging. The precipitates found in this work correspond well with the Y- and Nd-rich precipitates as observed in literature for alloy WE43 when processed with LPBF [Ref. 8], [Ref. 19] as well as for castings [Ref. 20], [Ref. 21].

In order to distinguish the grain and sub-grain boundaries, EBSD scans were performed on the cross-sections. Figure 12 shows an EBSD image of the cross-section and a very fine microstructure with homogeneously distributed equiaxed grains of around 2-4 µm in diameter can be observed. It is not possible to distinguish the melt pool borders, suggesting that the microstructure does not change at different locations within the melt pool. These observations were also made previously in literature of LPBF of WE43 [Ref. 8], [Ref. 19]. It should be noted that larger EBSD scans should be made in XY and XZ direction in order to have a more representative analysis of the grain structure and texture.

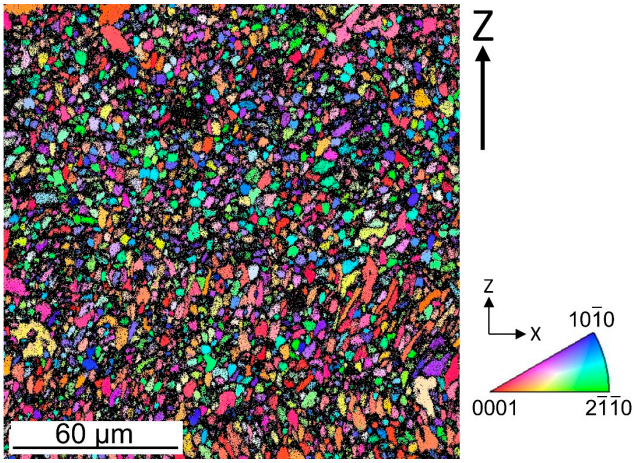

Figure 12: EBSD image of the cross-section along the Z direction

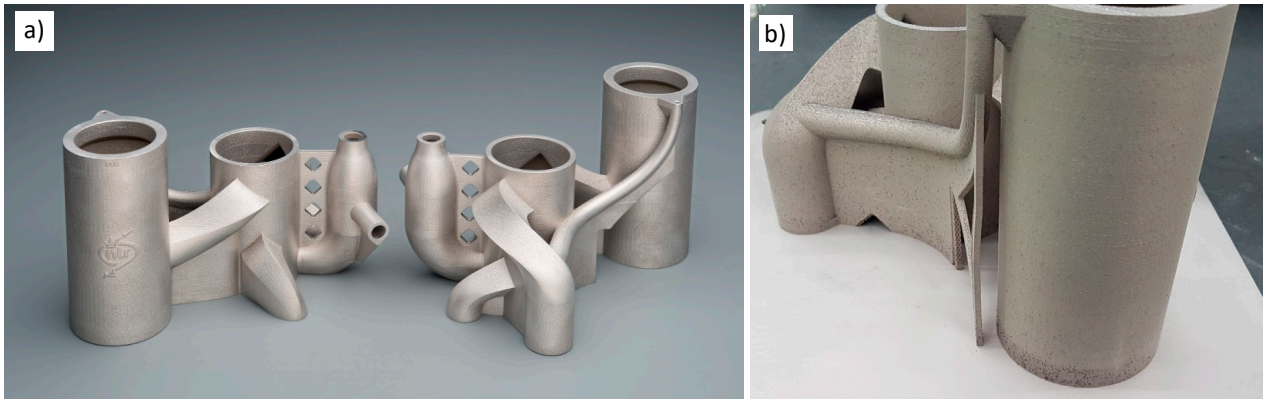

Figure 13: Magnesium AM demonstrators: a) overview of two demonstrators seen from the front and the back, b) a detail of a deformed support

4.4 LPBF production and evaluation of demonstrator parts

Figure 13 shows that the demonstrator parts were produced successfully. The as built surface roughness of the parts was relatively low and comparable to the roughness that was observed on the benchmark parts (Figure 9). Deformation of a support structure was observed. This indicates that residual stresses accumulated during the LPBF process.
Deviations from the CAD design, as measured with the GOM Atos 200 3D scanner, are shown in Figure 14. These deviations can be caused by either:

- Residual stresses that are introduced during LPBF production due to large thermal gradients. Deformations due to residual stresses were also observed on the benchmark part (Figure 9) and on a support structure under the demonstrator part (Figure 13).
- Material that is removed from the surfaces by sanding to further reduce the surface roughness.

A stress relief heat treatment was carried out in this study to reduce the influence of deformation after removal of the substrate plate. A heat treatment has a big influence on the final microstructure and subsequently on the corrosion resistance, mechanical performance and remaining residual stresses in the produced material. Common heat treatments for cast WE43 material such as T5 or T6 heat treatments are well investigated. The microstructure of a

LPBF material is very different from cast material. This means that well established heat treatments for cast WE43 are expected to be less suitable for WE43 produced by LPBF. It is therefore recommended to investigate which heat treatment should be applied on LPBF processed magnesium to obtain the required mechanical performance, corrosion resistance and minimum risk of deformation.

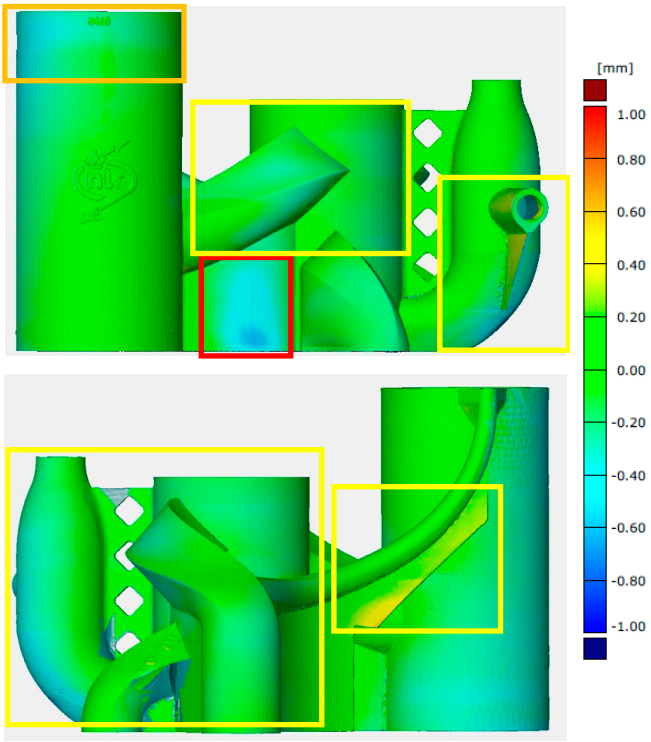

Figure 14: Deviations from the original CAD design measured using a GOM Atos 200

Simulation of deformations can be used to evaluate the design and the support structures. Exact elastic, plastic and thermal expansion properties are required for simulation of deformations. It is recommended to determine these values for LPBF material.

5 Conclusions

The objective of the research project, described in this paper, is to demonstrate the capability to produce high quality magnesium transmission housings with high complexity by LPBF. The following conclusions are drawn from this study:

- The evaluation of the magnesium powder that was used in this study indicated that a good processability could be expected for LPBF.
- An efficient optimization approach was applied that enabled selection of LPBF process parameters for the production of low porosity and roughness parts.
- SEM analysis showed a homogeneous microstructure at the melt pool and grain size scale. Some Y and Nd-rich precipitates were observed, which are typical for alloy WE43.
- LPBF of alloy WE43 results in very fine equiaxed grains, homogeneously distributed across the melt-pools.
- Some deformation occurred due to residual stresses. It is recommended to take the formation of residual stresses into account when designing parts and supports structures for LPBF of magnesium.
- No optimized heat treatment is available for printed magnesium material. It is recommended to develop a dedicated heat treatment for LPBF processed magnesium to obtain the required mechanical performance, corrosion resistance and minimum risk of deformation.
- It is recommended to determine elastic, plastic and thermal expansion properties of LPBF magnesium material for the simulation of deformations in order to evaluate and optimize the design and the support structures.

6 Acknowledgments

The authors would like to thank Boeing Phantom Works in Philadelphia PA for the confidence and support during this challenging research and development project. The authors also wish to thank Glenn Rossi and Robert Funk for the support during this collaboration. We are proud of what we have achieved and we could not have done that without this stimulating cooperation.

7 References

[1] L. Jauer, W. Meiners, and R. Poprawe, “Selective laser melting of biodegradable metals,” in *European congress and exhibition on powder metallurgy. European PM Conference Proceedings*, Hamburg, Germany, 2016, pp. 1–6.

[2] C. C. Ng, “Selective Laser Sintering of magnesium powder for fabrication of compact structures,” *2 C C Ng “Selective Laser Sinter. Magnes. Pow17th Int. Conf. Adv. Laser Technol.*, 2009.

[3] C. C. Ng, M. M. Savalani, H. C. Man, and I. Gibson, “Layer manufacturing of magnesium and its alloy structures for future applications,” *Virtual Phys. Prototyp.*, vol. 5, no. 1, pp. 13–19, Mar. 2010, doi: 10.1080/17452751003718629.

[4] C. C. Ng, M. M. Savalani, M. L. Lau, and H. C. Man, “Microstructure and mechanical properties of selective laser melted magnesium,” *Appl. Surf. Sci.*, vol. 257, no. 17, pp. 7447–7454, Jun. 2011, doi: 10.1016/j.apsusc.2011.03.004.

[5] B. Zhang, H. Liao, and C. Coddet, “Effects of processing parameters on properties of selective laser melting Mg–9%Al powder mixture,” *Mater. Des.*, vol. 34, pp. 753–758, Feb. 2012, doi: 10.1016/j.matdes.2011.06.061.

[6] M. Gieseke, C. Noelke, S. Kaierle, V. Wesling, and H. Haferkamp, “Selective Laser Melting of Magnesium and Magnesium Alloys,” in *Magnesium Technology 2013*, N. Hort, S. N. Mathaudhu, N. R. Neelameggham, and M. Alderman, Eds. Cham: Springer International Publishing, 2016, pp. 65–68.

[7] M. Gieseke, C. Nölke, S. Kaierle, H. J. Maier, and H. Haferkamp, “Selective Laser Melting of Magnesium Alloys for Manufacturing Individual Implants,” p. 6, 2014.

[8] M. Esmaily *et al.*, “A detailed microstructural and corrosion analysis of magnesium alloy WE43 manufactured by selective laser melting,” *Addit. Manuf.*, vol. 35, p. 101321, Oct. 2020, doi: 10.1016/j.addma.2020.101321.

[9] Z. Karaguiozova, A. Miteva, A. Ciski, and G. Cieślak, “Magnesium Application in Aerospace Industry,” in *12th Scientific Conference Space Ecology Safety*, Sofia, Bulgaria, 2016, pp. 2–4.

[10] Mathes John C., “Magnesium Alloys in the Aircraft Industry,” *Aircr. Eng. Aerosp. Technol.*, vol. 13, no. 11, pp. 323–326, Jan. 1941, doi: 10.1108/eb030844.

[11] E. Hombergsmeier, “Magnesium for aerospace applications,” 2nd international conference and exhibition “Magnesium—Broad Horizons,” 2007, pp. 1–13.

[12] Y. Henn and A. Fein, “Project MagForming -Development of new magnesium forming technologies for the aeronautics industry,” *Publ. Final Act. Rep.*, pp. 1–58, 2010.

[13] T. Kurzynowski, “The potential of SLM technology for processing magnesium alloys in aerospace industry,” *Arch. Civ. Mech. Eng.*, p. 13, 2020.

[14] A. Fein, “New method for producing magnesium alloy twin-rib aircraft brackets.,” Madrid, Spain, 2011, [Online]. Available: www.transportresearch.info/Upload/Documents/201211/20121102_140318_81319_Publishable_Final_Activity_Report.pdf.

[15] R. E. Śliwa *et al.*, “Metal Forming of Lightweight Magnesium Alloys for Aviation Applications,” vol. 62, no. No 3, 2017, [Online]. Available: http://journals.pan.pl/dlibra/docmetadata?id=105173 DOI - 10.1515/amm-2017-0239.

[16] M. Wojtas, A. Sobieszek, L. Czajkowski, and R. Żurawski, “Modern Materials in Aerospace Industry – Fatigue Tests of Magnesium Alloy Control System Lever of the Unmanned ILX–27 Helicopter,” in *30th Congress of the International Council of the Aeronautical Sciences*, Korea, 2016, pp. 25–30.

[17] J. Bogdanow and K. Szabelski, “Design of helicopter,” *Lub. Univ. Technol. Publ. Lub.*, 1991.

[18] Dziubinska Anna and Gontarz Andrzej, “A new method for producing magnesium alloy twin-rib aircraft brackets,” *Aircr. Eng. Aerosp. Technol. Int. J.*, vol. 87, no. 2, pp. 180–188, Jan. 2015, doi: 10.1108/AEAT-10-2013-0184.

[19] N. A. Zumdick, L. Jauer, L. C. Kersting, T. N. Kutz, J. H. Schleifenbaum, and D. Zander, “Additive manufactured WE43 magnesium: A comparative study of the microstructure and mechanical properties with those of powder extruded and as-cast WE43,” *Mater. Charact.*, vol. 147, pp. 384–397, Jan. 2019, doi: 10.1016/j.matchar.2018.11.011.

[20] S. Kandalam, P. Agrawal, G. S. Avadhani, S. Kumar, and S. Suwas, “Precipitation response of the magnesium alloy WE43 in strained and unstrained conditions,” *J. Alloys Compd.*, vol. 623, pp. 317–323, Feb. 2015, doi: 10.1016/j.jallcom.2014.09.179.

[21] T. Rzychoń and A. Kielbus, “Microstructure of WE43 casting magnesium alloy,” *J. Achiev. Mater. Manuf. Eng.*, vol. 21, pp. 31–34, Mar. 2007.

Dedicated to innovation in aerospace

Royal NLR - Netherlands Aerospace Centre

NLR operates as an objective and independent research centre, working with its partners towards a better world tomorrow. As part of that, NLR offers innovative solutions and technical expertise, creating a strong competitive position for the commercial sector.

NLR has been a centre of expertise for over a century now, with a deep-seated desire to keep innovating. It is an organisation that works to achieve sustainable, safe, efficient and effective aerospace operations.
The combination of in-depth insights into customers' needs, multidisciplinary expertise and state-of-the-art research facilities makes rapid innovation possible. Both domestically and abroad, NLR plays a pivotal role between science, the commercial sector and governmental authorities, bridging the gap between fundamental research and practical applications. Additionally, NLR is one of the large technological institutes (GTIs) that have been collaborating over a decade in the Netherlands on applied research united in the TO2 federation.

From its main offices in Amsterdam and Marknesse plus two satellite offices, NLR helps to create a safe and sustainable society. It works with partners on numerous programmes in both civil aviation and defence, including work on complex composite structures for commercial aircraft and on goal-oriented use of the F-35 fighter. Additionally, NLR helps to achieve both Dutch and European goals and climate objectives in line with the Luchtvaartnota (Aviation Policy Document), the European Green Deal and Flightpath 2050, and by participating in programs such as Clean Sky and SESAR.

For more information visit: **www.nlr.org**

Postal address
PO Box 90502
1006 BM Amsterdam, The Netherlands
e) info@nlr.nl **i)** www.nlr.org

Royal NLR
Anthony Fokkerweg 2
1059 CM Amsterdam, The Netherlands
p) +31 88 511 3113

Voorsterweg 31
8316 PR Marknesse, The Netherlands
p) +31 88 511 4444